Tensor-network approach to compute genuine multisite entanglement in infinite quantum spin chains

Sudipto Singha Roy,[1,2,3] Himadri Shekhar Dhar,[4,5] Aditi Sen(De),[3] and Ujjwal Sen[3]

[1]*Instituto de Física Téorica UAM/CSIC, C/ Nicolás Cabrera 13-15, Cantoblanco, 28049 Madrid, Spain*

[2]*Department of Applied Mathematics, Hanyang University (ERICA), 55 Hanyangdaehak-ro, Ansan, Gyeonggi-do, 426-791, Korea*

[3]*Harish-Chandra Research Institute, HBNI, Chhatnag Road, Jhunsi, Allahabad 211 019, India*

[4]*Institute for Theoretical Physics, Vienna University of Technology, Wiedner Hauptstraße 8-10/136, A-1040 Vienna, Austria*

[5]*Physics Department, Blackett Laboratory, Imperial College London, SW7 2AZ London, United Kingdom*

(Received 22 August 2018; published 6 June 2019)

We devise a method based on the tensor-network formalism to calculate genuine multisite entanglement in ground states of infinite spin chains containing spin-1/2 or spin-1 quantum particles. The ground state is obtained by employing an infinite time-evolving block decimation method acting upon an initial matrix product state for the infinite spin system. We explicitly show how such infinite matrix product states with translational invariance provide a natural framework to derive the generalized geometric measure, a computable measure of genuine multisite entanglement, in the thermodynamic limit of quantum many-body systems with both spin-1/2 and higher-spin particles.

DOI: 10.1103/PhysRevA.99.062305

I. INTRODUCTION

In recent years, entanglement [1] has turned out to be an important characteristic in the study of low-dimensional strongly correlated quantum systems, especially from the perspective of critical phenomena in the low-temperature regime of many quantum many-body systems [2–5] and implementation of quantum information protocols using solid-state, cold gas, and other physical substrates [6–10]. While most of the attention in studying these systems has been bestowed on bipartite entanglement measures such as entanglement of formation, concurrence, or block entanglement entropy, an important albeit difficult to estimate quantity is the multipartite entanglement in quantum many-body systems (see Ref. [1]). Interestingly, it has often been observed that there exist some cooperative phenomena where bipartite entanglement and other known order parameters fail to detect the interesting physics, which are then captured by multipartite entanglement [11–15]. Moreover, the study of multiparty entanglement in quantum systems with higher spins, even for finite-sized systems, remains largely unexplored.

When expanding the study of multipartite entanglement to understand complex quantum phenomena in the thermodynamic limit, for both spin-1/2 and higher-spin quantum particles, the innate difficulty is to characterize computable entanglement measures (for recent developments, see Refs. [11–21]). In most instances, for quantum many-body systems, the complexity in measuring multipartite entanglement scales exponentially with increasing dimension of the total Hilbert space, which in turn is associated with the number of quantum systems involved in the problem, and can often be unamenable even with approximate methods. In recent years, numerical techniques such as density matrix renormalization group (DMRG) [22], matrix product states (MPS) [23], and projected entangled pair states (PEPS) [24] have allowed unprecedented access to physical properties of many-body systems, including estimation of global entanglement in low-dimensional spin systems [11–13]. The growth of newer tensor-network methods [25], such as multiscale entanglement renormalization ansatz (MERA) [26], along with other significant developments in higher-dimensional [27] and topological quantum systems [28], provide newer directions to explore the role of multipartite entanglement in generic quantum systems.

In this work, we employ a tensor-network based approach to estimate the genuine multipartite entanglement, which for pure quantum states characterizes the situation where the many-body system cannot be formed by states that are products across some bipartition(s) of the multiparty system. We investigate this behavior in the thermodynamic limit of infinite chains of both spin-1/2 as well as spin-1 quantum systems. We show that matrix product states for infinite one-dimensional quantum spin systems provide a natural framework to estimate the *generalized geometric measure* (GGM) [19] (see also [16–18]), which is a computable measure of genuine multipartite entanglement, defined by using the geometry of the space of multiparty states. To demonstrate the efficacy of our formalism, we first consider a set of prototypical Hamiltonians of low-dimensional quantum spin systems. For instance, we obtain the ground states for spin-1/2 systems such as the transverse Ising and the *XYZ* models, using infinite time-evolving block decimation (*i*TEBD) [29] of an initial state. We show how the GGM in the thermodynamic limit of the system can be estimated from the final infinite matrix product state (*i*MPS). Subsequently, we extend our study to more complex models such as the spin-1 Ising model with transverse single-ion anisotropy. Here we observe that the genuine multipartite entanglement in the thermodynamic limit can clearly highlight the different quantum phases of

the many-body system and the scaling of entanglement can identify the critical points.

The paper is arranged as follows. After the brief introduction in Sec. I, we discuss GGM as a measure of genuine multiparty entanglement in Sec. II. We then look at how expressions for the reduced states can be obtained from the infinite MPS picture in Sec. III. In Sec. IV we look at how the ground states of spin chain models, containing spin-1/2 or spin-1 particles, can be derived using *i*TEBD. In Sec. V, we calculate the GGM for the ground states of these different models. We conclude with a discussion in Sec. VI.

II. GENERALIZED GEOMETRIC MEASURE

A hierarchy of geometric measures of multiparty entanglement [18] of an N-party pure quantum state, $|\Psi\rangle_N$, can be defined in terms of geometric distance between the given state and the set of k-separable states, $\mathcal{S}_k$, which is the set of all pure quantum states that are separable across at least $k-1$ partitions in the system or, alternatively, are a product of states of k subsystems. Considering fidelity subtracted from unity, which is closely connected to the Fubini-Study and the Bures metrics, as our choice of distance measure, one can define the geometric measure of multiparty entanglement as [16–19]

$$G_k(|\Psi\rangle_N) = 1 - \max_{|\chi\rangle\in\mathcal{S}_k} |\langle\chi|\Psi\rangle_N|^2, \tag{1}$$

where $2 \leqslant k \leqslant N$ and $|\langle\chi|\Psi\rangle_N|^2$ is the fidelity. The maximization ensures that G_k measures how entangled (or far away) a state $|\Psi\rangle_N$ is with respect to (from) the closest k-separable states. In principle, a set of $N-1$ measures of multipartite entanglement ($\{G_k\}$) can be defined, by employing the minimum distances from the $N-1$ sets, $\mathcal{S}_k$. Multipartite entanglement measures, such as the global entanglement [17], consider the distance of $|\Psi\rangle_N$ from the set of completely separable or N-separable states, $\mathcal{S}_{k=N}$. These measures do not detect separability that may occur across a lesser number of partitions ($k < N$). A more stringent measure is the genuine multipartite entanglement, $G_{k=2}$, which corresponds to the minimum distance from the set $\mathcal{S}_2$. Since $\mathcal{S}_k \subset \mathcal{S}_{k'}$, if $k' \leqslant k$, we get $\mathcal{S}_k \subset \mathcal{S}_2\, \forall\, k$. This implies that the minimal distance is computed by considering the minimization over all k-separable states for all k, and thus captures the presence of genuine multiparty entanglement in the quantum state. In other words, nonzero value of $G_{k=2}$, in Eq. (1), implies that $|\Psi\rangle_N$ is not separable across *any* bipartition.

In general, computation of G_k appears to be hard, as it involves maximization over a large set of k-separable states. Incidentally, $G_{k=2}$ for a quantum state is equal to the generalized geometric measure ($\mathcal{G}$) [19], which reduces to

$$\mathcal{G}(|\Psi\rangle_N) = 1 - \max_{\mathcal{S}_{\mathcal{A}:\mathcal{B}}} \left\{\lambda^2_{\mathcal{A}:\mathcal{B}} | \mathcal{A}\cup\mathcal{B} = \{N\}, \mathcal{A}\cap\mathcal{B} = \emptyset\right\}, \tag{2}$$

where $\mathcal{S}_{\mathcal{A}:\mathcal{B}} = \mathcal{S}_2$ is the set of all biseparable states, with bipartitions $\mathcal{A}$ and $\mathcal{B}$, and $\lambda_{\mathcal{A}:\mathcal{B}} = \max\{\lambda^i_{\mathcal{A}:\mathcal{B}}\}$ for the Schmidt decomposition, $|\Psi\rangle_N = \sum_i \lambda^i_{\mathcal{A}:\mathcal{B}} |\phi^i\rangle_{\mathcal{A}} |\tilde{\phi}^i\rangle_{\mathcal{B}}$. Here N denotes the set of N parties possessing the state $|\Psi\rangle_N$. The maximization over all k-separable states is reduced to optimization over the set of $\lambda^2_{\mathcal{A}:\mathcal{B}}$ across all possible bipartitions of $|\Psi\rangle_N$. Such simplification of $\mathcal{G}(|\psi\rangle_N)$ helps to evaluate genuine multiparty entanglement content of a multiparty state involving an arbitrary number of parties and in arbitrary dimensions. Note, however, that with increasing N the number of possible choices of the bipartitions also increases exponentially and hence computation of $\mathcal{G}$ becomes cumbersome. In addition to this, if the quantum state of the system cannot be defined uniquely, it is also not possible to compute the value of $\mathcal{G}$ for the system.

We present a brief outline of the proof for GGM ($\mathcal{G}$) being a measure of genuine multipartite entanglement [19] in the Appendix A. Importantly, we now show that the measure of $\mathcal{G}$ can be characterized in the language of tensor-network methods. In particular, we consider the MPS formalism in translationally invariant (TI) quantum systems, which provides a natural framework to estimate genuine multisite entanglement.

III. ANALYTICAL FORM OF REDUCED DENSITY MATRICES

The maximum Schmidt coefficient across a bipartition required for GGM is the square root of the maximum eigenvalue of the reduced density matrix of the subsystems across the bipartition. Obtaining the reduced density matrices of an infinite-sized system, using the MPS formalism, is the primary motivation of the paper. Let us begin with the preliminary MPS representation of a many-body quantum state, $|\Psi\rangle_N$, given by [24,25]

$$|\Psi\rangle_N = \sum_{i_1 i_2\cdots_N} \sum_{\alpha_2\ldots\alpha_{N-1}} \mathrm{Tr}\left(A^{i_1}_{\alpha_1,\alpha_2} A^{i_2}_{\alpha_2\alpha_3}\ldots A^{N}_{\alpha_{N-1}\alpha_N}\right) \times |i_1, i_2, i_3, \ldots, i_N\rangle, \tag{3}$$

where i_k is the physical index, with the local system dimension d, and α_k being the auxiliary index, each with a bond dimension D. $\{A^{i_k}\}$ are thus $D\times D$ matrices corresponding to each k site. For low values of D, the MPS representation of $|\Psi\rangle_N$ is very efficient as the number of parameters required to express the state scales with N as ND^2d, instead of d^N. This can be further reduced by considering some potential symmetry in the system, such as translational invariance of $\{A^{i_k}\}$ matrices. Importantly, in order to obtain the reduced density matrices of a quantum many-body system, one should be able to efficiently compute the $\{A^{i_k}\}$ matrices. However, there are only a few cases for which the exact MPS form of the quantum state is known [24,25]. One such example is the unnormalized N-qubit Greenberger-Horne-Zeilinger (GHZ) [30] state, $|\mathrm{GHZ}\rangle_N = |0\rangle^{\otimes N} + |1\rangle^{\otimes N}$, which is local unitarily equivalent to the possible entangled ground state of the Ising chain at large coupling strength [31]. For $D=2$ (and $d=2$ for qubits), the matrices for the MPS are $\{A^{i_k}\} = \{A^0(k), A^1(k)\} = \{\sigma^+\sigma_x, \sigma^-\sigma_x\}, \forall\, k$, where σ_k's are the usual Pauli matrices and $\sigma^\pm = \frac{1}{2}(\sigma_x \pm i\sigma_y)$. We note that the A^{i_k} matrices are translationally invariant. Another example of TI systems is the ground state of the AKLT Hamiltonian [32], where for $d=3$ and $D=2$, $\{A^{i_k}\} = \{A^0(k), A^1(k), A^2(k)\} = \{\sigma_z, \sqrt{2}\sigma^+, -\sqrt{2}\sigma^-\}, \forall\, k$. However, in general, the matrices $\{A^{i_k}\}$ can have explicit site dependence. For example, consider the N-qubit W state [33], $|W\rangle_N = \frac{1}{\sqrt{N}}(|10\ldots0\rangle + |01\ldots0\rangle + \cdots |00\ldots1\rangle)$, which is known to be the ground state of the ferromagnetic XX model with strong transverse field. Interestingly, although the state is translationally

invariant, the $\{A^{i_k}\}$ matrices are not, as shown for $D = 2$. Here, $\{A^0(k), A^1(k)\} = \{\sigma^+, \mathbb{I}_2\}$, for $k < N$, and $\{A^0(k), A^1(k)\} = \{\sigma^+\sigma_x, \sigma_x\}$, for $k = N$, where $\mathbb{I}_2$ is the 2×2 identity matrix [34].

In general, for MPS with site-dependent $\{A^{i_k}\}$, calculation of reduced density matrices of quantum states beyond moderate-sized systems may require considerable computational effort, especially if the bond dimension D is not small. This is a significant roadblock in the computation of GGM. However, if the system is TI, i.e., $\{A^{i_k}\} = A^i, \forall k$, and the A^i matrices can be efficiently estimated, then the reduced density matrices can be obtained even for infinite sized systems, thus allowing us to compute the genuine multipartite entanglement of quantum states in the thermodynamic limit. Let us begin with an MPS representation of a TI quantum system with local dimension d and $\{A^i\}$, with bond dimension D. The MPS could be obtained as a ground state of a physical Hamiltonian or a time-evolved quantum state, quenched from some initial product state. To calculate the reduced density matrices, we first consider the case for single-site reduced state first from the multiqubit TI MPS. For a very small system size, viz. $N = 2$, and known A^i matrices, the expression for the single-site reduced density matrix is given by $\rho^1 = \frac{1}{E^2}$ $\mathrm{tr}[(A^0 \otimes \bar{A}^0)E]|0\rangle\langle 0| + \mathrm{tr}[(A^0 \otimes \bar{A}^1)E]|0\rangle\langle 1| + \mathrm{tr}[(A^1 \otimes \bar{A}^0)$ $E]|1\rangle\langle 0| + \mathrm{tr}[(A^1 \otimes \bar{A}^1)E]|1\rangle\langle 1|$, where $E = \sum_i A^i \otimes \bar{A}^i$ is the transfer matrix of the translationally invariant system and $\bar{A}$ is the conjugate transpose of A. Similarly, for $N = 3$, $\rho^1 =$ $\frac{1}{E^3}\mathrm{tr}[(A^0 \otimes \bar{A}^0)E^2]|0\rangle\langle 0| + \mathrm{tr}[(A^0 \otimes \bar{A}^1)E^2]|0\rangle\langle 1| + \mathrm{tr}[(A^1 \otimes$ $\bar{A}^0)E^2]|1\rangle\langle 0| + \mathrm{tr}[(A^1 \otimes \bar{A}^1)E^2]|1\rangle\langle 1|$. For an arbitrary N and local dimension, $d = 2$ (qubit), the expression for the single-site density matrix is given by

$$\rho^1 = \sum_{i,j=0}^{1} \frac{\mathrm{tr}[(A^i \otimes \bar{A}^j)E^{N-1}]}{E^N} |i\rangle\langle j|. \tag{4}$$

At this stage, our aim is to generalize Eq. (4) for very large and, eventually, infinite systems. To this end, we first consider the spectral decomposition of the transfer matrix, in the MPS formalism for infinite system, known as *i*MPS, $E^N = \sum_i \lambda_i^N |L^i\rangle\langle R^i|$, where $|L^i\rangle$ and $|R^i\rangle$ are the left and right eigenvectors, respectively. For $N \to \infty$, E has 1 as a nondegenerate eigenvalue and all other eigenvalues have modulus smaller than 1, i.e., $E^N = |L^0\rangle\langle R^0| + \sum_{j=2}^{D^2} \lambda_k^N |L^k\rangle\langle R^k|$. Hence, as $N \to \infty$, $E^N \to |L^0\rangle\langle R^0|$. Thus the elements of ρ^1, as expressed in Eq. (4), are given by

$$\rho^1_{ij} = \frac{\langle L^0|A^i \otimes \bar{A}^j|R^0\rangle}{\langle L^0|R^0\rangle}. \tag{5}$$

Similarly, one can obtain the form of all m-consecutive site $l, l+1, l+2, \ldots$ $(m \geqslant 2)$ reduced density matrices, using the relation

$$\rho^m_{ij} = \frac{\langle L^0|A^{i_1}A^{i_2}\ldots A^{i_m} \otimes \bar{A}^{j_1}\bar{A}^{j_2}\ldots\bar{A}^{j_m}|R^0\rangle}{\langle L^0|R^0\rangle}, \tag{6}$$

where $i = i_1 i_2 \ldots i_m$ and $j = j_1 j_2 \ldots j_m$. For nonconsecutive sites, $l, l + r_1, l + r_1 + r_2, \ldots$ the expression of the m-site reduced density matrix is given by

$$\rho^m_{ij} = \frac{\langle L_0|\tilde{A}^1 E^{r_1-1}\tilde{A}^2 E^{r_2-1}\ldots\tilde{A}^m|R_0\rangle}{\langle L^0|R^0\rangle},$$

where $\tilde{A}^k = (A^{i_k} \otimes \bar{A}^{j_k})$.

This has remarkable significance as the number of parameters required to represent the m-site density matrices is reduced from d^m to $D^2 d$. The reduced density matrix can thus be used to estimate the genuine multisite entanglement in systems described using infinite MPS.

IV. GROUND-STATE MPS USING *i*TEBD

We briefly describe the algorithm to simulate the ground state of an infinite, one-dimensional quantum many-body Hamiltonian, $\mathcal{H}$, using the infinite MPS formalism. We start with an arbitrary MPS, $|\Psi\rangle_N$, as expressed in Eq. (3), and then eventually build the ground state *i*MPS using an infinite time-evolving block decimation method. To this end, starting from $|\Psi\rangle_N$, we perform an imaginary time evolution: $|\Psi\rangle_N \to e^{-\tau\mathcal{H}}|\Psi\rangle_N$. The ground-state configuration $|\Psi_0\rangle_N$ is then obtained when τ becomes very large, i.e., $|\Psi\rangle_N \sim |\Psi_0\rangle_N + \sum_{i=1}^{d^N} e^{-\tau(E_i - E_0)}|\Psi_i\rangle_N \xrightarrow{\tau\to\infty} |\Psi_0\rangle_N$. In order to perform the *i*TEBD, we first use second-order Suzuki-Trotter (ST) decomposition [35] on the exponential unitary operation and express each term in the TI matrix product operator (MPO) form [36,37]. This essentially helps to change the optimization problem of the energy for the total system to the optimization associated with each decomposed TI MPO. After one such ST iteration, we obtain an MPS, $|\Psi^t\rangle$, which, in general, has a bigger bond dimension than the initial MPS. Therefore, one needs to truncate this to the allowed bond dimension D. We then normalize the imaginary time evolved state and choose that as a seed for the next time iteration. After each such ST step, energy per site $(E_0/N = \frac{1}{N}\langle\Psi^t|\mathcal{H}|\Psi^t\rangle)$ is calculated and the expressions of the $\{A^i\}$ matrices for the *i*MPS of the ground state of the given Hamiltonian are then obtained by minimizing the energy. In general, energy per site scales with the size of the system. However, through some intermediary steps, one can show that, for $N \to \infty$, it converges to E_∞ (say). Hence the final $\{A^i\}$ matrices are obtained when the energy per site converges.

To apply the above *i*MPS formalism we begin with a one-dimensional quantum system consisting of spin-1/2 particles. Such a quantum many-body Hamiltonian can be written, with a certain degree of genericity, as

$$\mathcal{H} = \sum_{\langle ij\rangle} \left(J_x S_i^x S_j^x + J_y S_i^y S_j^y + \Delta S_i^z S_j^z\right) + \sum_i h S_i^z, \tag{7}$$

where J_x, J_y are the coupling constants along x and y directions, respectively, Δ is the "anisotropy" along the z direction, h is the strength of the transverse field, $S^k = \sigma_k$ are the Pauli spin matrices, and $\langle ij\rangle$ denotes the nearest-neighbor sites. Two important models that can be derived from $\mathcal{H}$ are the transverse Ising (in the limit $J_y = \Delta = 0$) and the anisotropic *XYZ* model ($J_{x(y)} = J \pm \gamma$ and $h = 0$) [38–40]. Note that, in the limit $\gamma = 0$, the *XYZ* model reduces to the anisotropic *XXZ* model, which has gained some attention in studies on strongly correlated systems [41]. We note that, in recent years,

cooperative phenomena in quantum spin chains have been widely explored in the context of quantum information theory, especially in terms of entanglement [2–5] and other quantum correlations [42].

We next look at the *i*MPS representation for more complex quantum spin systems. For instance, we consider a quantum many-body chain with higher-spin particles, viz. the spin-1 Ising model with a transverse field akin to parameters arising from single-ion anisotropy generated by crystal fields [43]. These systems can also be considered to be a derivative of the Blume-Emery-Griffiths model [44], where the quadratic terms have been neglected. Such models have lately been used to study phase transitions in multicomponent fluids and semiconductor systems [45]. The Hamiltonian of the spin-1 model is thus given by

$$\bar{\mathcal{H}} = \mathcal{J}_z \sum_{\langle ij \rangle} \mathcal{S}_i^z \mathcal{S}_j^z + \mathcal{K}\left(\mathcal{S}_i^x\right)^2, \tag{8}$$

where $\mathcal{S}^i$'s are generalizations of the Pauli matrices for a spin-1 system, $\mathcal{J}_z$ denotes the coupling along the z direction, and $\mathcal{K}$ denotes the strength of the single-ion anisotropy parameter due to the crystal field in the transverse direction. The model undergoes a quantum phase transition at $\frac{\mathcal{J}_z}{\mathcal{K}} = 2$ [43].

In implementing the *i*MPS form and the *i*TEBD algorithm for obtaining the ground state of these Hamiltonians, we fix the bond dimension at $D = 10$ and choose the initial Trotter step to be $\tau = 10^{-2}$, which is then gradually changed to 10^{-6} to improve accuracy. The convergence of the ground-state energy is determined with an accuracy 10^{-6}. Once the ground state *i*MPS is obtained, one can access the Schmidt coefficients across all possible bipartitions of the quantum state by contracting the tensors efficiently, as shown in Eq. (6). The behavior of genuine multisite entanglement in ground-state phases of the Hamiltonian, in the thermodynamic limit, can then be estimated from the generalized geometric measure.

V. GENUINE MULTISITE ENTANGLEMENT IN THE THERMODYNAMIC LIMIT

For the transverse Ising model, we consider a region away from critical point ($h/J_x = 1$), viz. $1.1 \leqslant h/J_x \leqslant 2$. The variation of GGM ($\mathcal{G}$) with respect to the transverse field strength h/J_x is depicted in Fig. 1. The thermodynamic limit of the genuine multisite entanglement, in the infinite spin lattice, is compared with the corresponding values obtained for finite-sized lattices ($N = 8$, 10, and 12) using exact diagonalization. In order to compute the value of GGM ($\mathcal{G}$) using an exact diagonalization method, in all the cases ($N = 8$, 10, 12), we perform the optimization in Eq. (2) by taking into account all possible bipartitions [whose number is $\sum_{i=1}^{6} \binom{N}{i}$ for $N = 12$]. We note that, for the transverse field Ising model, maximum value of Schmidt coefficient always comes from the single-site reduced density matrices. We use this fact to compute the value of GGM ($\mathcal{G}$) in the thermodynamic limit using *i*MPS. Therefore, in our case, Eq. (4) will serve the purpose. For this model, in the region parametrized by $0 \leqslant h/J_x \leqslant 0.8$, the energy gap closes and as discussed earlier, it is not possible to compute the multiparty entanglement using the measure GGM for nonunique ground states. The figure shows a distinct

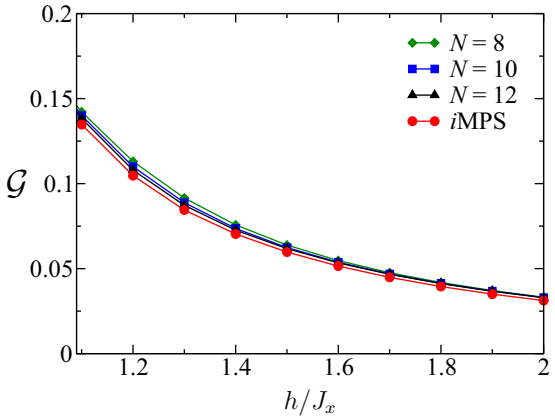

FIG. 1. Variation of GGM ($\mathcal{G}$) with field strength (h) for the transverse Ising model, for different one-dimensional lattice sizes, viz. $N = 8$ (green diamonds), 10 (blue squares), 12 (black triangles), and infinite N (red circles). Both axes represent dimensionless quantities.

scaling of $\mathcal{G}$ at field strengths closer to the critical point, $h/J_x = 1$. In this region, the difference between the GGM ($\mathcal{G}$) values, obtained using exact diagonalization method ($N = 12$) and *i*MPS, turns out to be at most $\approx 10^{-3}$. Away from it, $\mathcal{G}$ quickly becomes scale invariant, and approaches its thermodynamic limit even for low N. Here, the difference between the GGM ($\mathcal{G}$) values computed for $N = 12$ and *i*MPS becomes $\lesssim 10^{-4}$.

Let us now consider the *XYZ* Hamiltonian in absence of magnetic field, i.e., $J_x, J_y, \Delta \neq 0$, $h = 0$. The behavior of $\mathcal{G}$ with Δ/J, for the anisotropic *XYZ* Hamiltonian with $\gamma = 0.5$, is depicted in Fig. 2. Unlike the Ising case, from the exact diagonalization results for this model, we note that the maximum value of Schmidt coefficient always comes from the consecutive two-site reduced density matrices. We again use this result to compute the value of GGM in the thermodynamic limit using *i*MPS. Therefore, in this case, we use Eq. (6) for computation of the maximum Schmidt coefficients. As in the Ising case, here also degeneracy hinders us to find a

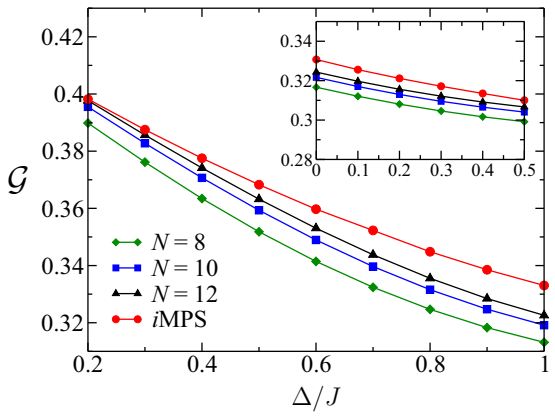

FIG. 2. Variation of GGM ($\mathcal{G}$) with Δ/J for the *XYZ* model with $\gamma = 0.5$, for different one-dimensional lattice sizes. Both axes represent dimensionless quantities. In the inset we plot the same quantities for $\gamma = 0$ case (*XXZ* model).

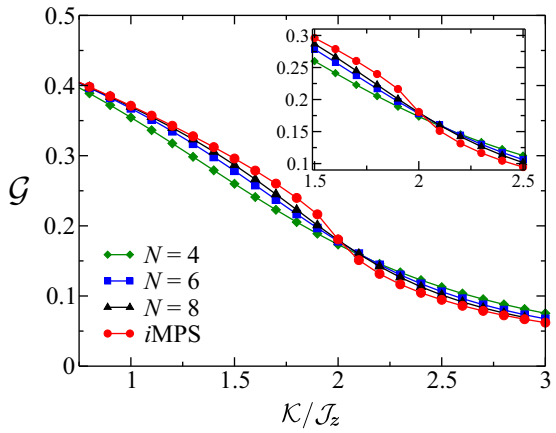

FIG. 3. Variation of GGM ($\mathcal{G}$) with $\frac{\mathcal{K}}{\mathcal{J}_z}$ for the spin-1 model described in Eq. (8), for different one-dimensional lattice sizes, viz. $N = 4$ (green diamonds), 6 (blue squares), 8 (black triangles), and infinite N (red circles). Both axes represent dimensionless quantities. In the inset, we show the GGM in the region close to the transition point ($\frac{\mathcal{K}}{\mathcal{J}_z} \approx 2$).

unique ground state for the region $-1 \leqslant \Delta/J \leqslant 0$. Therefore, for this model, we consider the following region between two critical points, for both finite and infinite lattices, parametrized by $0.2 \leqslant \Delta/J \leqslant 1.0$. Figure 2 shows that in contrast to the transverse Ising model, no scale invariance is achieved for $\mathcal{G}$ even away from the critical points, and it is not possible to achieve the thermodynamic limit by exactly diagonalizing a spin model with small system size. In this case, the difference between the GGM values computed for $N = 12$ and iMPS at small values of Δ/J becomes $\lesssim 10^{-3}$, which further increases to $\lesssim 10^{-2}$ as Δ/J tends to 1. For the XXZ model ($\gamma = 0$) (see the inset of Fig. 2), where the critical points are known to exist in the vicinity of $\Delta/J = \pm 1$, a similar absence of scale invariance is observed. Here the difference between the GGM values computed for $N = 12$ and iMPS never decreases below 10^{-3}. Thus iMPS plays a significant role in computing genuine multipartite entanglement in these systems.

We now look at the genuine multipartite entanglement properties of the more complex higher-spin model, viz. the spin-1 Ising model with single-ion anisotropy as expressed in Eq. (8). We note that, in contrast to the spin-1/2 models, behavior of multipartite entanglement in this spin-1 model is unexplored even for finite spin systems. Here, we look at the behavior of GGM in the thermodynamic limit of the system using the iMPS formalism. The behavior of genuine multiparty entanglement is plotted in Fig. 3. We again note that, like the transverse Ising model, the maximum Schmidt coefficient in this case also comes from the single-site reduced density matrices. Moreover, as in the previous cases, we observe that GGM starts decreasing monotonously with the increase of the strength of the single-ion anisotropy or the crystal field. However, for the spin-1 model, the scaling pattern of GGM in the thermodynamic limit shows several interesting features. For instance, before $\mathcal{K} < 2$, in most of the regions, GGM increases with system size. On the other hand, for $\mathcal{K} > 2$, the trend is reversed, i.e., the value of GGM decreases with the increase of N. However, the variation of GGM with the anisotropy parameter clearly detects the critical points in the system. We observe that, near the value $\mathcal{K} \approx 2$, GGM becomes almost scale invariant, which is a known value at which quantum phase transition occurs in the system. Therefore, our study shows that the scaling of GGM can identify the vital characteristics of the critical phenomena in the spin-1 model.

VI. DISCUSSION

In this work, we have shown how the tensor-network approach provides a natural structure to study genuine multiparty entanglement, quantified by generalized geometric measure, in many-body quantum systems. In particular, the method involved matrix product states to efficiently obtain the reduced density matrices of infinite quantum spin lattices, which upon making use of symmetries such as translational invariance of the matrices allowed us to accurately estimate the generalized geometric measure of systems consisting of both spin-1/2 and higher spins. The method thus provided us a viable theoretical framework to look at interesting cooperative and critical phenomena by investigating multiparticle physical quantities in the thermodynamic limit of quantum many-body systems.

Importantly, this approach to compute generalized geometric measure using tensor networks is in principle also applicable for higher-dimensional lattices, provided the relevant tensors under the iMPS formalism are accessible using available numerical techniques. Finally, we also note that the formalism presented in the work may provide useful directions in investigating genuine multipartite entanglement properties in several quantum systems, including condensed-matter, photonic, and other topological systems, where tensor-network methods have turned out to be successful in studying physical properties.

ACKNOWLEDGMENTS

The research of S.S.R. was supported in part by the INFOSYS scholarship for senior students. H.S.D. acknowledges funding by the Austrian Science Fund (FWF), Project No. M 2022-N27, under the Lise Meitner programme of the FWF.

APPENDIX: PROOF OF GGM AS A MEASURE OF GENUINE MULTIPARTY ENTANGLEMENT

Here, we present a very concise proof for the GGM to be a measure of genuine multiparty entanglement, starting from the concept of k separability and the definition of the geometric measures of multiparty entanglement in Eq. (1). An important point to note is that G_2 is the minimum distance from the set of all k-separable quantum states, $\mathcal{S}_k \forall k$. However, in principle, as measurements over general entangled bases yield higher or equal values as compared to those over product bases, the maximum fidelity in Eq. (1) can always be considered from the set $\mathcal{S}_k$ with lowest k, as they contain more clustered partitions. Hence, for G_2, the set $\mathcal{S}_2$ of biseparable states contains a closest separable state. Let $\{\lambda^i_{\mathcal{A}:\mathcal{B}}\}_{i=1}^d$ and $\{|\phi^i\rangle_\mathcal{A}, |\tilde{\phi}^i\rangle_\mathcal{B}\}_{i=1}^d$ be the set of real, nonnegative Schmidt coefficients and corresponding orthogonal

vectors, respectively, across the bipartition $\mathcal{A} : \mathcal{B}$, where $d = \max\{d_\mathcal{A}, d_\mathcal{B}\}$. A biseparable state, in general, can be written as $|\chi\rangle = |\eta\rangle_\mathcal{A}|\tilde{\eta}\rangle_\mathcal{B}$. The fidelity is then given by

$$|\langle\chi|\Psi\rangle_N| = \left|\sum_i \lambda^i_{\mathcal{A}:\mathcal{B}}\langle\eta|\phi^i\rangle_\mathcal{A}\langle\tilde{\eta}|\phi^i\rangle_\mathcal{B}\right| = \left|\sum_i \lambda^i_{\mathcal{A}:\mathcal{B}} f^i_\mathcal{A}\, g^i_\mathcal{B}\right|. \tag{A1}$$

A value of fidelity, possibly nonmaximal, corresponds to $|\eta\rangle_\mathcal{A} = |\phi^k\rangle_\mathcal{A}$ and $|\tilde{\eta}\rangle_\mathcal{B} = |\tilde{\phi}^k\rangle_\mathcal{B}$, such that $f^k_\mathcal{A} = g^k_\mathcal{B} = 1$, where k gives $\lambda_{\mathcal{A}:\mathcal{B}} = \lambda^k_{\mathcal{A}:\mathcal{B}} = \max\{\lambda^i_{\mathcal{A}:\mathcal{B}}\}$. Thus we have $|\langle\chi|\Psi\rangle_N| \geqslant \lambda_{\mathcal{A}:\mathcal{B}}$. However,

$$|\langle\chi|\Psi\rangle_N| \leqslant \sum_i \lambda^i_{\mathcal{A}:\mathcal{B}}|f^i_\mathcal{A}||g^i_\mathcal{B}| \leqslant \lambda_{\mathcal{A}:\mathcal{B}}\sum_i |f^i_\mathcal{A}||g^i_\mathcal{B}| \leqslant \lambda_{\mathcal{A}:\mathcal{B}},$$

where we have used the triangle law for absolute values and the relations $\sum_i \lambda_{\mathcal{A}:\mathcal{B}} \geqslant \sum_i \lambda^i_{\mathcal{A}:\mathcal{B}}$ and $\sum_i |f^i_\mathcal{A}||g^i_\mathcal{B}| \leqslant 1$. This gives us the desired relation $|\langle\chi|\Psi\rangle_N| = \lambda_{\mathcal{A}:\mathcal{B}} = \max\{\lambda^i_{\mathcal{A}:\mathcal{B}}\}$. For all biseparable states, $|\chi\rangle$, $\lambda_{\mathcal{A}:\mathcal{B}} = 1$, and as expected $\mathcal{G}(|\Psi\rangle_N) = 0$. From Eq. (2), we see that the maximum among the real and positive Schmidt coefficient squared, across all possible bipartitions, subtracted from unity gives the GGM, which measures the genuine multipartite entanglement in the system.

[1] R. Horodecki, P. Horodecki, M. Horodecki, and K. Horodecki, Quantum entanglement, Rev. Mod. Phys. **81**, 865 (2009).

[2] A. Osterloh, L. Amico, G. Falci, and R. Fazio, Scaling of entanglement close to a quantum phase transition, Nature (London) **416**, 608 (2002).

[3] T. J. Osborne and M. A. Nielsen, Entanglement in a simple quantum phase transition, Phys. Rev. A **66**, 032110 (2002).

[4] L. Amico, R. Fazio, A. Osterloh, and V. Vedral, Entanglement in many-body systems, Rev. Mod. Phys. **80**, 517 (2008).

[5] M. Lewenstein, A. Sanpera, V. Ahufinger, B. Damski, A. Sen (De), and U. Sen, Ultracold atomic gases in optical lattices: mimicking condensed matter physics and beyond, Adv. Phys. **56**, 243 (2007); M. Lewenstein, A. Sanpera, and V. Ahufinger, *Ultracold Atoms in Optical Lattices: Simulating Quantum Manybody Systems* (Oxford University Press, Oxford, 2012).

[6] B. E. Kane, A silicon-based nuclear spin quantum computer, Nature (London) **393**, 133 (1998).

[7] R. Raussendorf and H. J. Briegel, A One-Way Quantum Computer, Phys. Rev. Lett. **86**, 5188 (2001); H. J. Briegel, D. E. Browne, W. Dür, R. Raussendorf, and M. Van den Nest, Measurement-based quantum computation, Nat. Phys. **5**, 19 (2009).

[8] A. Kitaev, Fault-tolerant quantum computation by anyons, Ann. Phys. (NY) **303**, 2 (2003); C. Nayak, S. H. Simon, A. Stern, M. Freedman, and S. Das Sarma, Non-Abelian anyons and topological quantum computation, Rev. Mod. Phys. **80**, 1083 (2008).

[9] S. Bose, Quantum Communication through an Unmodulated Spin Chain, Phys. Rev. Lett. **91**, 207901 (2003); V. Subrahmanyam, Entanglement dynamics and quantum-state transport in spin chains, Phys. Rev. A **69**, 034304 (2004).

[10] D. P. DiVincenzo, D. Bacon, J. Kempe, G. Burkard, and K. B. Whaley, Universal quantum computation with the exchange interaction, Nature (London) **408**, 339 (2000).

[11] T.-C. Wei, D. Das, S. Mukhopadyay, S. Vishveshwara, and P. M. Goldbart, Global entanglement and quantum criticality in spin chains, Phys. Rev. A **71**, 060305(R) (2005).

[12] R. Orús, Universal Geometric Entanglement Close to Quantum Phase Transitions, Phys. Rev. Lett. **100**, 130502 (2008); R. Orús and T.-C. Wei, Visualizing elusive phase transitions with geometric entanglement, Phys. Rev. B **82**, 155120 (2010); Q.-Q. Shi, R. Orús, J. O. Fjærestad, and H.-Q. Zhou, Finite-size geometric entanglement from tensor network algorithms, New J. Phys. **12**, 025008 (2010).

[13] C.-Y. Huang and F.-L. Lin, Multipartite entanglement measures and quantum criticality from matrix and tensor product states, Phys. Rev. A **81**, 032304 (2010).

[14] M. N. Bera, R. Prabhu, A. S. De, and U. Sen, Multisite entanglement acts as a better indicator of quantum phase transitions in spin models with three-spin interactions, arXiv:1209.1523 [quant-ph].

[15] A. Biswas, R. Prabhu, A. Sen (De), and U. Sen, Genuine-multipartite-entanglement trends in gapless-to-gapped transitions of quantum spin systems, Phys. Rev. A **90**, 032301 (2014).

[16] A. Shimony, Degree of entanglement, Ann. N.Y. Acad. Sci. **755**, 675 (1995); H. Barnum and N. Linden, Monotones and invariants for multi-particle quantum states, J. Phys. A **34**, 6787 (2001).

[17] T.-C. Wei and P. M. Goldbart, Geometric measure of entanglement and applications to bipartite and multipartite quantum states, Phys. Rev. A **68**, 042307 (2003).

[18] M. Blasone, F. DellAnno, S. DeSiena, and F. Illuminati, Hierarchies of geometric entanglement, Phys. Rev. A **77**, 062304 (2008).

[19] A. Sen (De) and U. Sen, Channel capacities versus entanglement measures in multiparty quantum states, Phys. Rev. A **81**, 012308 (2010); Bound Genuine Multisite Entanglement: Detector of Gapless-Gapped Quantum Transitions in Frustrated Systems, arXiv:1002.1253; G. D. Chiara and A. Sanpera, Genuine quantum correlations in quantum many-body systems: A review of recent progress, Rep. Prog. Phys. **81**, 074002 (2018).

[20] T. R. de Oliveira, G. Rigolin, M. C. de Oliveira, and E. Miranda, Multipartite Entanglement Signature of Quantum Phase Transitions, Phys. Rev. Lett. **97**, 170401 (2006); M. Hofmann, A. Osterloh, and O. Gühne, Scaling of genuine multiparticle entanglement close to a quantum phase transition, Phys. Rev. B **89**, 134101 (2014).

[21] H. S. Dhar, A. Sen (De), and U. Sen, Characterizing Genuine Multisite Entanglement in Isotropic Spin Lattices, Phys. Rev. Lett. **111**, 070501 (2013); The density matrix recursion method: Genuine multisite entanglement distinguishes odd from even quantum spin ladder states, New J. Phys. **15**, 013043 (2013); S. Singha Roy, H. S. Dhar, D. Rakshit, A. Sen (De), and U. Sen, Diverging scaling with converging multisite entanglement

in odd and even quantum Heisenberg ladders, *ibid.* **18**, 023025 (2016); Analytical recursive method to ascertain multisite entanglement in doped quantum spin ladders, Phys. Rev. B **96**, 075143 (2017).

[22] S. R. White, Density Matrix Formulation for Quantum Renormalization Groups, Phys. Rev. Lett. **69**, 2863 (1992); U. Schollwöck, The density-matrix renormalization group in the age of matrix product states, Ann. Phys. (N.Y.) **326**, 96 (2011).

[23] M. Fannes, B. Nachtergaele, and R. F. Werner, Finitely correlated states on quantum spin chains, Commun. Math. Phys. **144**, 443 (1992); S. Östlund and S. Rommer, Thermodynamic Limit of Density Matrix Renormalization, Phys. Rev. Lett. **75**, 3537 (1995); J. Dukelsky, M. A. Martín-Delgado, T. Nishino, and G. Sierra, Equivalence of the variational matrix product method and the density matrix renormalization group applied to spin chains, Europhys. Lett. **43**, 457 (1997).

[24] F. Verstratete, J. I. Cirac, and V. Murg, Matrix product states, projected entangled pair states, and variational renormalization group methods for quantum spin systems, Adv. Phys. **57**, 143 (2008).

[25] J. I. Cirac and F. Verstraete, Renormalization and tensor product states in spin chains and lattices, J. Phys. A **42**, 504004 (2009); J. Eisert, *Emergent Phenomena in Correlated Matter*, Series on Modeling and Simulation, edited by E. Pavarini, E. Koch, and U. Schollwöeck (Jülich Research Centre, Jülich, Germany, 2013); R. Órus, A practical introduction to tensor networks: matrix product states and projected entangled pair states, Ann. Phys. (N.Y.) **349**, 117 (2014).

[26] G. Vidal, Class of Quantum Many-Body States That Can Be Efficiently Simulated, Phys. Rev. Lett. **101**, 110501 (2008); G. Evenbly and G. Vidal, Tensor network states and geometry, J. Stat. Phys. **145**, 891 (2011).

[27] F. Verstraete and J. I. Cirac, Renormalization algorithms for quantum-many body systems in two and higher dimensions, arXiv:cond-mat/0407066; J. Jordan, R. Orús, G. Vidal, F. Verstraete, and J. I. Cirac, Classical Simulation of Infinite-Size Quantum Lattice Systems in Two Spatial Dimensions, Phys. Rev. Lett. **101**, 250602 (2008).

[28] N. Bultinck, D. J. Williamson, J. Haegeman, and F. Verstraete, Fermionic matrix product states and one-dimensional topological phases, Phys. Rev. B **95**, 075108 (2017); W.-T. Xu and G.-M. Zhang, Matrix product states for topological phases with parafermions, *ibid.* **95**, 195122 (2017).

[29] G. Vidal, Efficient Simulation of One-Dimensional Quantum Many-Body Systems, Phys. Rev. Lett. **93**, 040502 (2004).

[30] D. M. Greenberger, M. A. Horne, and A. Zeilinger, in *Bell's Theorem, Quantum Theory, and Conceptions of the Universe*, edited by M. Kafatos (Kluwer Academic, Dordrecht, The Netherlands, 1989).

[31] P. Stelmachovic and V. Buzek, Quantum-information approach to the Ising model: Entanglement in chains of qubits, Phys. Rev. A **70**, 032313 (2004).

[32] I. Affleck, T. Kennedy, E. H. Lieb, and H. Tasaki, Rigorous Results on Valence-Bond Ground States in Antiferromagnets, Phys. Rev. Lett. **59**, 799 (1987).

[33] A. Zeilinger, M. A. Horne, and D. M. Greenberger, in *Proceedings of Squeezed States and Quantum Uncertainty*, edited by D. Han, Y. S. Kim, and W. W. Zachary, NASA Conf. Publ. **73**, 3135 (1992); W. Dür, G. Vidal, and J. I. Cirac, Three qubits can be entangled in two inequivalent ways, Phys. Rev. A **62**, 062314 (2000); A. Sen (De), U. Sen, M. Wiesniak, D. Kaszlikowski, and M. Zukowski, Multiqubit W states lead to stronger nonclassicality than Greenberger-Horne-Zeilinger states, *ibid.* **68**, 062306 (2003).

[34] D. Perez-Garcia, F. Verstraete, M. M. Wolf, and J. I. Cirac, Matrix product state representations, Quantum Inf. Comput. **7**, 401 (2007).

[35] H. F. Trotter, On the product of semi-groups of operators, Proc. Am. Math. Soc. **10**, 545 (1959); M. Suzuki, Generalized Trotter's formula and systematic approximants of exponential operators and inner derivations with applications to many-body problems, Commun. Math. Phys. **51**, 183 (1976); Fractal decomposition of exponential operators with applications to many-body theories and Monte Carlo simulations, Phys. Lett. A **146**, 319 (1990).

[36] V. Murg, J. I. Cirac, B. Pirvu, F. Verstraete, Matrix product operator representations, New J. Phys. **12**, 025012 (2010).

[37] B. Pirvu, Ph.D. thesis, University of Vienna, 2012.

[38] S. Sachdev, *Quantum Phase Transitions*, 2nd ed. (Cambridge University Press, Cambridge, UK, 2011).

[39] N. Goldenfeld, *Lectures on Phase Transitions and the Renormalization Group* (Addison-Wesley, New York, 1992).

[40] S. L. Sondhi, S. M. Girvin, J. P. Carini, and D. Shahar, Continuous quantum phase transitions, Rev. Mod. Phys. **69**, 315 (1997); M. Vojta, Quantum phase transitions, Rep. Prog. Phys. **66**, 2069 (2003).

[41] J. Abouie, A. Langari, and M. Siahatgar, Thermodynamic behavior of the XXZ Heisenberg s=1/2 chain around the factorizing magnetic field, J. Phys.: Condens. Matter **22**, 216008 (2010); B. B. Orrs, M. Weyrauch, and M. V. Rakov, Phase diagram of one-, two-, and three-dimensional quantum spin systems derived from entanglement properties, Quantum Inf. Comput. **16**, 0885 (2016).

[42] K. Modi, A. Brodutch, H. Cable, T. Paterek, and V. Vedral, The classical-quantum boundary for correlations: Discord and related measures, Rev. Mod. Phys. **84**, 1655 (2012).

[43] N. C. Eddeqaqi, M. Saber, A. El-Atri, and M. Kerouad, Phase diagram of spin-1 Ising model in a transverse crystal field, Physica A **272**, 144 (1999); J. Oitmaa and A. M. A. von Brasch, Spin-1 Ising model in a transverse crystal field, Phys. Rev. B **67**, 172402 (2003); Z. H. Yang, L. P. Yang, H. N. Wu, J. Dai, and T. Xiang, Exact solutions of a class of $S = 1$ quantum Ising spin models, *ibid.* **79**, 214427 (2009).

[44] M. Blume, V. J. Emery, and R. B. Griffiths, Ising model for the λ transition and phase separation in He^3-He^4 mixtures, Phys. Rev. A **4**, 1071 (1971).

[45] C. Ekiz and M. Keskin, Multicritical phase diagrams of the Blume-Emery-Griffiths model with repulsive biquadratic coupling including metastable phases, Phys. Rev. B **66**, 054105 (2002).